

# Web-based 3D Smog Visualization for Air Pollution Analysis

1<sup>st</sup> Jordan Limperis

Department of Computer Science  
Georgia Southern University  
Statesboro, Georgia  
jl29293@georgiasouthern.edu

2<sup>nd</sup> Felix Hamza-Lup

Department of Computer Science  
Georgia Southern University  
Statesboro, Georgia  
fhamzalup@georgiasouthern.edu

3<sup>rd</sup> Weitian Tong\*

Department of Computer Science  
Georgia Southern University  
Statesboro, Georgia  
wtong.research@gmail.com

**Abstract**—The increase in the transaction of data and availability of augmented reality devices (virtual, augmented, and mixed reality) have led to the formation of a suitable environment for the real-time communication of complex air pollution data to a diverse population of individuals. In recent years, air pollution has become a global concern and thus it is important to constantly monitor air pollution and communicate it to citizens. In this study we design a web-based, 3-Dimensional virtual reality platform to portray air pollution risk through a realistic smog effect over the Joshua Tree Landscape. Through user natural language processing evaluation, this platform is shown to increase user risk perception of air pollution and its relation to environmental landscapes. Our model promotes the user's exploration of an air pollution landscape and provides tools to portray air pollution data to citizens.

**Index Terms**—3D Visualization, 3D Modelling, X3DOM, Web Cartography

## I. INTRODUCTION

Data visualization is a powerful tool that helps comprehending and discovering patterns in data. A fundamental step after data collection and analysis is data presentation to support the user's decision-making process. To understand relationships among variables, discover hidden patterns, information (i.e. processed data) out to be to be presented in an easy-to-understand manner. We perceive up to 80% of all information around us by means of sight [1]. Hence, data visualization techniques empower experts and laymen alike to understand and interpret data. Advances in data visualization have enabled users to reconstruct the past and discover patterns in the present. Data visualization has revolutionized fields such as architecture, medicine [2], finance [3], education [4], and E-commerce [5]. Presently, most modern geospatial data visualization occurs in a 2-dimensional (2D) space, which has introduced challenges to data interpretation. The inability to communicate current system or expected system state in a meaningful format is a formidable challenge, and as big data has grown, state description is further derived from more data sources. The diversity and wealth of data available makes concise fusion of data for the empowerment of stakeholders a daunting task. 2D graphical maps fail to capture the context

of heterogeneous, diverse data sources where both temporal and spatial characteristics are vital to understanding. With large scale sensor networks becoming increasingly prevalent [6], more data than ever is available and 3-Dimensional (3D) visualization and visualization sharing are becoming excellent tools for digesting such complex data streams.

New technologies in cartographic representation, or geovisualization techniques, have enabled cartographers to display interactive 3D models. These models incorporate all details on an extra dimension thus giving the viewer a deeper understanding of the scene, and thus overcoming existing visualization barriers. By enticing users to explore a generated world through appealing interaction, these models raise the awareness of citizens to the patterns within big data. This appeal has led to several projects on various societal issues and their associated data sources. One such area of interest is in the complex issue of air pollution and the rich information available in air quality data [7]. By enabling users to explore complex geographic data scenes, 3D visualization systems empower experts and laymen alike to discover potential solutions, and thus make complex information available to a wider audience [8]. These tools reach out to a broad audience making it easy for anyone to use maps and browse through geodata.

3D maps are interactive by nature and are to be designed so they can be explored by the user [9]. The exploration of scenes needs to allow for the increasing data wealth and further knowledge, which is not easily achieved, especially in geology [10]. Consequentially, 3D visualization systems must comply with high standards regarding aesthetic, technical and usability aspects [11]. Complex geological 3D data usually requires expert software, like ArcGIS, to display. Widespread use of comparable displays within Web browsers has not been achieved in the field of geology, despite the advantages of such systems [12]. The increasing intersection and need for a standard system to display and share information over the web led to the historical development of the standard City Geography Markup Language (CityGML). This standard is a catalytic for 3D models to exchange and information presentation, with a specific focus on city landscapes [13], [14]. Originally, these geographical information systems (GIS) were integrated with the Virtual Reality Modelling Language (VMRL97) and deployed on the World Wide Web (WWW).

**Type of submission:** Full/Regular Research Paper

**Symposium:** CSCI-RTCS

**Corresponding author** (\*): Weitian Tong, wtong.research@gmail.com

The evolution of VMRL97 led to the development of the superior eXtensible 3D (X3D) standard, empowering users to share and develop 3D content and applications directly in the web browsers in combination with the Hypertext Markup Language (HTML5) frameworks [15]. The X3D open standard is built upon the World Wide Web Consortium (W3C) eXtensible Markup Language (XML) standard. X3D enables the development of applications targeting big data visualization and pattern extraction. By delivering 3D content over the web, it furthers our goal of increased access for geospatial data to all stakeholders.

The rest of the paper is structured as follows. In Section 2 we provide an overview of the current state of art in Web-based 3D visualization. In section 3 we summarize our core research question and rationale. In section 4 we illustrate our 3D model architecture and construction of a visual scene. In section 5

## II. RELATED WORK

To establish 3D models of territorial landscapes, it is essential to consider acquisition of topographical data for representation of Digital Terrain Models (DTM). Regarding visual fidelity of these models, Jobst et al. [16] mention possible problems including object occlusion, perspective distortion, the existence of a multitude of scales in one view, and the lack of comparability of objects' geometry. The ability to use geospatially, well registered geometry, and geospatially informed data structures was recognized as vital for overcoming 3D model usability issues [17]. The X3D geospatial component, designed with a geospatial node to overcome these limitations, occupies a unique space between the world of GIS's and 3D computer graphics. Normally, GIS's treat 3D display as an extra feature instead being equally important to coordinate map systems. Even though modern GIS systems (ArcGIS or PostGIS, for example) have a coordinate system, they remain map tools based on a 2D world view for the analysis and visualization of geospatial information [17]. On the other hand X3D was specifically designed to deal with the challenges associated with 3D structure. Examples of these datasets and analytical areas include:

- Urban planning and visibility analysis [18], [19]
- Crisis management and flood visualization [20], [21], [22]
- Noise Mapping [23], [7]
- Air flight and unmanned aerial vehicles [24]
- Meteorological and atmospheric analysis [25], [7]

Another benefit of the X3D standard is openness, no necessity of proprietary licensing, unlike ArcGIS. By being a web-enabled ISO open standard, barriers to utilization are removed. In fact, X3D is the only open standard available that provides robust support for real-time rendering of 3D graphics [26]. An open-source tool furthers the research goal of enabling experts and laymen alike to utilize X3D as a 3D cartographic tool. With growing pressure for vendors to use open standards rather than closed proprietary tools [27], X3D is a clear choice in the development of a 3D cartographic tool free of proprietary licensing. With the World Health Organization attributing 4.2



Fig. 1. Smog causing reduced visibility from Key's View, Joshua Tree Park, blanketing the Coachella Valley [32].

million deaths to pollution globally, air quality is an important area of research [28]. Epidemiological studies have established that exposure to  $PM_{2.5}$ , or particles with diameters less than  $2.5 \mu m$ , is strongly associated with many negative health effects [29], [30]. Specifically in California, the California State University showed that air pollution costs the state 28 billion dollars a year, and consequentially California is rife with air pollution awareness efforts and research [31]. For example, the Environmental Protection Agency (EPA) has deployed an extensive network of air pollution monitoring sites across the United States. Despite these efforts, air pollution's negative effects continue to persist even in areas of ecological risk, like Joshua Tree National Park [32]. An important atmospheric phenomenon important for nature reserves like Joshua Tree is smog (illustrated in Figure 1). Due to the smog's reactions to high temperatures, air pollution has strong negative effects on Joshua trees (*Yucca brevifolia*). Smog also affects soils, surface waters, and human health. Moreover, the National Park Service found that visibility is reduced from 160 to 55 miles when heavy smog is present. This study seeks to replicate realistic smog effects over the Joshua Tree landscape to increase public awareness of pollution issues while also overcoming the limitations of current GIS's to show informed, accurate geospatial features in a web-enabled 3D space [32].

To better understand the atmospheric processes using air quality simulations, José et al. [7] proposed several tools to represent 3D atmospheric effects with geographic data. Their work targeted experts, scientists, as well as the public. Their assortment of tools included the ability to change the color of the 3D virtual world terrain as an atmospheric indicator. They integrated their tools with a 3D model from Google Earth. They found that augmented reality (AR) raises the level of immersion felt by users interacting with air pollution data. Prophet et al. [33] furthered this research by studying the increase in awareness due to AR in the context of air pollution. Their project of asking the user to plant a tree in their 3D world encourages users to understand how pollution affects

them. They concluded 3D virtual worlds are very appealing for scientific data visualization since they enabled users to perform collaborative data exploration and analysis. With the far-reaching success of 3D visualization of geographical scenes in conjunction with geospatial data, there is great opportunity to better disseminate information about the effects of air pollution on local environments and increase public awareness. With classical air quality information dissemination showing muted effects on public perception [34], it is vital to explore modern web-based 3D approaches to air pollution visualization. With smog being an established ecological model with negative local effects [35], we aim to address a gap in 3D data visualization of portraying realistic smog effects as it would reduce actual visual acuity. Haeberling et al. [36] evaluated sky structure and haze density as a 3D cartographic design principal. They found that the addition of haze improves depth perception of the user, giving the scene a more realistic effect. With a more realistic 3D model, the perception of risk increases which is significantly positive in predicting attitude and behavioral intention [37]. To our knowledge, this is the first study implementing realistic smog effects with the goal of spurring smog-reduction behaviors. We hope that our web-based 3D model of Joshua Tree Park’s atmospheric smog effects is a boon in promoting ecological awareness of the risks of smog on local ecological resources.

### III. POLLUTION AND GEOGRAPHIC DATA INTEGRATION

The prime aim of this research is to support decision making regarding air pollution and its risk to the Joshua Tree National park as pollution level varies annually. Air Quality Index (AQI) data, elevation data, and satellite imagery are integrated into the open source, web-based X3D framework to create a realistic 3D map of Joshua Tree with smog as an air pollution effect. We go beyond a 2D portrayal of Joshua Tree to show how smog effects would be perceived in a realistic scenario using non-planar X3D elements. The workflow starts with gathering publicly available data to recreate the 3D scene of Joshua Tree, as well as its associated smog levels. Using this data, we implement a 3D GIS environment using the X3D standard and then match air quality readings from various sensors throughout the 2021 year to visual acuity within our X3D scene. In Figure 2 we illustrate our system design with implementation of heterogeneous data sources into an X3D framework.

#### A. Air Quality Index Data

For pollution data, Air Quality Index (AQI) as determined by the Environmental Protection Agency is employed. AQI indicates the degree of air pollution, the potential health effects from air pollution and enables the public understand localized air quality levels. The EPA calculates AQI based on the concentration of major air pollutants like ground-level  $O^3$ ,  $PM_{2.5}$ ,  $PM_{10}$ , carbon monoxide, nitrogen dioxide, and nitrogen oxide. AQI is reported by a six-color scheme corresponding from good to hazardous air quality as shown in Figure 3.

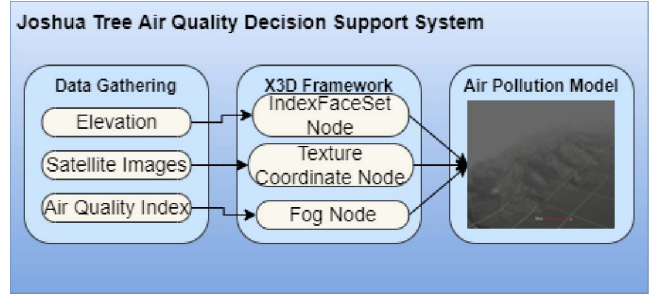


Fig. 2. Conceptual scheme of system design

AQI	Health Concern	Color	Explanation
0-50	Good	Green	Clean air, no health risk
51-100	Moderate	Yellow	Light air pollution, little health risk
101-150	Unhealthy for sensitive groups (USG)	Orange	Only sensitive groups are affected
151-200	Unhealthy	Red	Unhealthy air for everyone
201-300	Very Unhealthy	Purple	Serious health effects for everyone
301-500	Hazardous	Maroon	Severe adverse health effects, even death

Fig. 3. United States AQI Standard [38].

AQI maps, published by the EPA, show air quality across a mapping area using the six-color scheme and are used for AQI reporting and forecasting. For example, [airnow.gov](http://airnow.gov) provides near real-time hourly AQI maps for the United States and major cities. Within Joshua Tree National Park there is a air pollutant monitoring station tracking pollutant levels since 2018. AQI maps provide a good visualization of air quality and its localized effect on human health, but research shows that risk perception based on the six-color scale is limited [39]. Because of the lack of risk perception associated with this public communication scheme, we build upon the work of Zhu et al. [37] to better illustrate the risk of air pollution by using smog as a visual indicator over a realistic terrain map of Joshua Tree Park. We implement a realistic geographical model of the Pinto Basin of Joshua Tree National Park which is between two mountain ranges in an alluvial fan, a place where sediments gather carried by water. This ecology supports plant growth and makes the Ocotillo Patch, a nature preserve within the designated area. The flora of this area attracts tourists for a sweeping panoramic view of Joshua Tree [40]. Since this area is a popular tourist location, visual occlusion by smog would impact user perception of the Joshua Tree health. Our implementation employs elevation data provided by Google Earth to recreate a realistic terrain map [41]. Google Earth uses a Digital Elevation Model (DEM) gathered by NASA Shuttle Radar Topography Mission [42]. The elevation data spans an area of approximately 18 square kilometers. Elevation spans approximately 600 to 1200 meters above sea level. To achieve a high-fidelity landscape, Google Earths satellite is employed imagery to overlay a realistic texture over the coordinate elevation data [41]. Google Earth collects continuous images collected by satellites orbiting the Earth; the satellite images are sourced from a variety of satellite companies and are

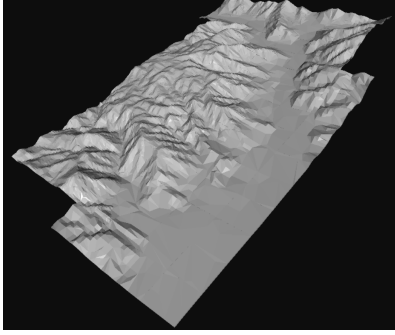


Fig. 4. The Polygonal Mesh of the Pinto Basin at Joshua Tree Park

gathered on varying scales, from days to years. The satellite networks included in Google Earth satellite image dataset include Landsat, MODIS, and sentinel [43]. We divide Google Earth’s satellite imagery into approximately  $108m^2$  squares to tile onto our elevation data. It is important to note that all our data sources are open source and publicly available to ensure our air pollution decision support system remains available to all users without proprietary limitations.

### B. X3D Implementation

X3D has substantial geospatial functionality which we utilize for implementation of Google Earth elevation data and satellite imagery. We also utilize new X3D atmospheric effect nodes to create realistic smog associated with EPA AQI data. In X3D scenes, the XZ plane is considered horizontal and the +Y direction points vertically upwards.

#### 1) Generating the Joshua Tree Park Surface Morphology:

To integrate our Google Earth elevation data for Joshua Tree we use the X3D IndexedFaceSet Node, which specifies an abstract 3D shape composed of a structured set of polygons with any number of edges. The IndexedFaceSet node uses the X3D Coordinate node to specify the vertices and edges for an abstract polygon [44]. This node is equivalent to triangular irregular networks (TINs) in standard GIS software [45]. We employ the IndexedFaceSet node to digitally represent Joshua Tree Park surface morphology. The vertices of the elevation data are connected with a set of edges to form a network of triangles that capture the position of elevation features, like ridges. These shapes can be irregular and thus capture variable slope gradients. There are various methods of interpreting elevation data to form these the triangular mesh, such as Delaunay triangulation [45]. We employed the BlenderGIS add-on for Blender as it is both open source and follows known standards using Delaunay triangulation. BlenderGIS uses the Flip algorithm where a triangulation of points is created and then the edges are flipped until no triangle is non-Delaunay, or such that no point is inside the circumcircle of any triangle [46]. The process is repeated 158 times over the  $108m^2$  square grids to create a mesh of the Joshua Tree Pinto Basin as illustrated in Figure 4.

2) *Surface texture Integration:* Building upon the Indexed-FaceSet Node, the TextureCoordinate X3D Node is used to

$$\begin{bmatrix} x_e \\ y_e \\ z_e \\ w_e \end{bmatrix} = \begin{bmatrix} \text{Camera} \\ \text{View} \\ \text{Matrix} \end{bmatrix} \begin{bmatrix} \text{Modeling} \\ \text{Matrix} \end{bmatrix} \begin{bmatrix} x_0 \\ y_0 \\ z_0 \\ w_0 \end{bmatrix}$$

Fig. 5. Transformation of object coordinates and associated textures into the viewing plane of the user [47]

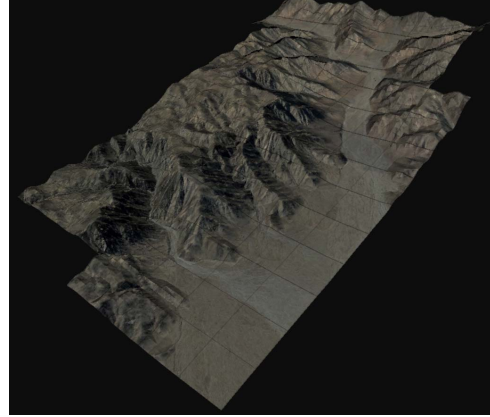


Fig. 6. Texture integration Google satellite imagery and Joshua Tree Park polygonal mesh.

specify a set of 2D texture Coordinate to overlay Google satellite imagery, in order to map the Google satellite imagery to the associated vertices. Projective texture mapping (PTM) lets the Google satellite imagery texture be projected in the volume seen from a particular X3D viewpoint or a camera position. Projective texturing was originally designed by Kim et al. [47] and Kamburelis et al. [48] by materializing shadow mapping, which we utilize in the BlenderGIS add-on. Furthermore, the Google satellite images are parsed into separate components to map them to each individual terrain mesh square in a pattern. Using the original formulation specified by Everitt et al. [49], object coordinates are transformed into the view frustum by equation 5.

Additional variables come into play such as projection point, direction, and aspect ratio. Utilizing this method, we implement the TextureCoordinate Node to create a textured scene of the Joshua Tree Pinto Basin as illustrated in Figure 6.

3) *Realistic Smog Modeling based on AQI Data:* The X3D Fog node [44] employs a simple visual trick of mixing a fog color to emulate a reduction in visual depth. Vital to this design, we implement a smog control user interface (UI) with a simple slider bar to control the visibilityRange field to emulate varying levels of smog in the scene. This field specifies the distance in length base units (in the world coordinate system) at which objects are completely obscured by fog [44]. We implement our slider bar UI for control of the fog employing a basic UI provided by X3D architecture [44]. Through this implementation, the user is capable of controlling the smog level. Additionally, it furthers the research goal of instilling a sense of risk in the user’s perception of the

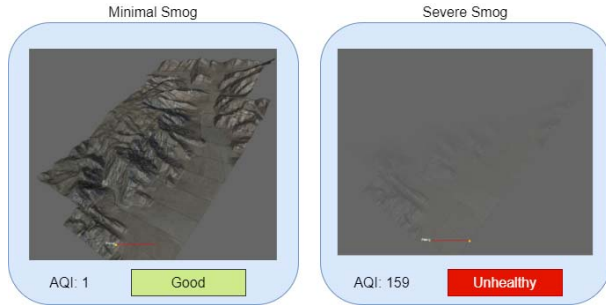


Fig. 7. Range of smog levels on the realistic Joshua Tree landscape.

effects of air pollution through a perceivable visual effect. This perception of risk and ability to see a visual effect of the smog allows the user to discern better relationships in the Air Quality Index data. To evaluate the efficacy of our model in increasing user risk perception of air pollution, a short interview questionnaire was created to qualitatively evaluate the users' perceptions. This data is then illustrated through a word processing algorithm to display for this research; the details of this method are presented in Interpretation of Results section.

National Park Service (NPS) data shows that when heavy smog is present, visual acuity of Joshua Tree viewpoints can be reduced from 160 to 55 miles. To effectively exhibit this reduction in visual acuity to the user through a realistic smog, we map this long-range reduction in view distance to a reduced scale for our small scale model to account for limitations in view length of 3D models. We map this range from 30 to 5 units within the visibilityRange field to correspond respectively for minimal smog to severe smog as emphasized in Figure 7. The maximum record AQI for Joshua Tree was 159 (on June 27, 2018) in the first year of monitoring, which corresponds to an unhealthy level for all individuals. This vast and fluctuating difference in AQI levels and levels of effects on the user, as well as the environment can now be easily communicated with an easy-to-understand visual signal of a realistic smog effect. By mapping these pollution levels to an easy-to-understand 3D model available freely on the Web, the user can discern patterns within the data. Since 2018, the levels of maximum AQI have decreased from 159 to 105 in 2021 with a clustering around summer months due to pollution's correlative relationship with temperature. Using the visualization system, the user does not need to comprehend complex noisy data, but they can simply visualize in the Web-browser an interactive topographical scene and quickly gain a deep understanding of the pollution's effects on the environment due to smog.

#### IV. SIMULATION EVALUATION AND RESULTS INTERPRETATION

To effectively evaluate the perception of risk of the user after interaction with the Joshua Tree smog simulation, a pre-post experimental design is created. In air pollution research, asking

open-ended questions has shown to elicit greater contextual information about air pollution risk perception [50]. To build upon existing research, this study performs the following pre-post experimental survey design to gather key ideas of the users' perception of risk on air pollution. The design of the survey is modeled after an established clean air initiative for Asian cities, which gained widespread use and can act as a data foundation for air pollution risk perception research [51]. Users are encouraged to give in-depth responses to ensure that an appropriate perception is gathered by the survey questions.

Questions asked prior to viewing interactive Joshua Tree smog simulation. User response is gathered through a recording and then transferred to text.

- How is the overall air quality in your city compared to last year?
- What do you think causes air pollution?

Questions asked after interacting with the Joshua Tree smog simulation. A short introduction of Joshua Tree ecology and AQI data is presented in combination with the smog simulation.

- How do you think air pollution in your city will change in the future?
- How can local governance help improve air quality?

A total of five participants were surveyed for this pre-post experimental design. The recorded responses of the participants are transferred to textual data using Google Cloud's speech to text application, which has shown to be accurate in translation [52]. Using the keyword generation and display algorithm of Kimura et al. [52], the important points of the survey responses are extracted and gathered in an easy-to-understand word-web display. In Figure 8 the responses of the participants are gathered and displayed in a word-web. Across all five participants, air pollution had a strong association with "smoke" and the user's personal opinions ("think") on the issue. Knowledge of the subject encapsulated key words, like "Global Warming". There was a trend to think that "companies" were a main cause of air pollution due to their "manufacturing" as well as peoples' use of "cars" when "driving". There was no indication of perception of ecological impacts of air pollution and their risks. There was a minority trend to think that air pollution might be "fake" or "naturally" occurring, but others thought that air pollution was "important". These illustrate the diverse perception of air pollution across participants.

In Figure 9 the responses of the participants are gathered and displayed after interaction with the Joshua Tree smog simulation. Across the five participants, there was a consistency in voicing personal opinion ("think") on air pollution issues. One of the most significant changes in responses was the acknowledgement of contextual information, like "smog", "California", and "Joshua," which the users might have not been aware of prior to interaction. "Information" regarding air pollution became a central topic of their responses indicating recognition of the information displayed. This means that the



- [8] L. Herman, A. Křnová, J. Russnák, and T. Řezník, "Comparison of standard-and proprietary-based approaches to detailed 3d city mapping," in *Modern Trends in Cartography*. Springer, 2015, pp. 131–144.
- [9] A. M. MacEachren, "An evolving cognitive-semiotic approach to geographic visualization and knowledge construction," *Information Design Journal*, vol. 10, no. 1, pp. 26–36, 2001.
- [10] M.-J. Kraak, "The role of the map in a web-gis environment," *Journal of Geographical Systems*, vol. 6, no. 2, pp. 83–93, 2004.
- [11] H. Lorenz, M. Trapp, and J. Döllner, "Interaktive, multiperspektivische ansichten für geovirtuelle 3d-umgebungen," *KN-Journal of Cartography and Geographic Information*, vol. 59, no. 4, pp. 175–181, 2009.
- [12] F. Von Reumont, J. J. Arsanjani, and A. Riedl, "Visualization of geologic geospatial datasets through x3d in the frame of webgis," *International Journal of Digital Earth*, vol. 6, no. 5, pp. 483–503, 2013.
- [13] T. H. Kolbe, "Representing and exchanging 3d city models with citygml," in *3D geo-information sciences*. Springer, 2009, pp. 15–31.
- [14] G. Gröger, T. H. Kolbe, A. Czerwinski, and C. Nagel, "OpenGIS city geography markup language (citygml) encoding standard, version 1.0.0," 2008.
- [15] F. Silva, D. Gutierrez, J. Rodríguez, and M. Figueiredo, "A web3dgis framework using citygml and x3d," 2011.
- [16] M. Jobst and T. Germachis, "The employment of 3d in cartography—an overview," *Multimedia cartography*, pp. 217–228, 2007.
- [17] A. Plesch and M. McCann, "The x3d geospatial component: X3dom implementation of georigin, geolocation, geoviewpoint, and geoposition-interpolator nodes," in *Proceedings of the 20th International Conference on 3D Web Technology*, 2015, pp. 31–37.
- [18] J. Ki, "Developing a geospatial web-gis system for landscape and urban planning," *International Journal of Digital Earth*, vol. 6, no. 6, pp. 580–588, 2013.
- [19] C. Guney, S. A. Girginkaya, G. Cagdas, and S. Yavuz, "Tailoring a geomodel for analyzing an urban skyline," *Landscape and Urban Planning*, vol. 105, no. 1-2, pp. 160–173, 2012.
- [20] T. Bandrova, S. Zlatanova, and M. Konecny, "Three-dimensional maps for disaster management," in *ISPRS Annals of the Photogrammetry, Remote Sensing and Spatial Information Sciences, Volume 1-2, XXII ISPRS Congress, August-September 2012, pp. 19-24*. International Society for Photogrammetry and Remote Sensing, 2012.
- [21] S. Kemec, S. Duzgun, S. Zlatanova, D. Dilmen, and A. Yalciner, "Selecting 3d urban visualisation models for disaster management: Fethiye tsunami inundation case," in *Proc. 3rd Int. Conf. Cartogr. GIS, Nessebar, Bulgaria*, 2010, pp. 1–9.
- [22] L. Herman and T. Reznik, "3d web visualization of environmental information-integration of heterogeneous data sources when providing navigation and interaction," *The International Archives of Photogrammetry, Remote Sensing and Spatial Information Sciences*, vol. 40, no. 3, p. 479, 2015.
- [23] C.-w. Law, C.-k. Lee, A. S.-w. Lui, M. K.-l. Yeung, and K.-c. Lam, "Advancement of three-dimensional noise mapping in hong kong," *Applied Acoustics*, vol. 72, no. 8, pp. 534–543, 2011.
- [24] T. Řezník, B. Horáková, and R. Szturc, "Geographic information for command and control systems," in *Intelligent Systems for Crisis Management*. Springer, 2013, pp. 263–275.
- [25] J. Congote, A. Moreno, L. Kabongo, J.-L. Pérez, R. San-José, and O. Ruiz, "Web based hybrid volumetric visualisation of urban gis data-integration of 4d temperature and wind fields with lod-2 citygml models," *Usage, Usability, and Utility of 3D City Models—European COST Action TU0801*, p. 03001, 2012.
- [26] L. Daly and D. Brutzman, "X3d: Extensible 3d graphics standard [standards in a nutshell]," *IEEE Signal Processing Magazine*, vol. 24, no. 6, pp. 130–135, 2007.
- [27] R. Arnaud and T. Parisi, "Developing web applications with collada and x3d," *White paper*, 2007.
- [28] (2019) Stop denying the risks of air pollution. [Online]. Available: <https://doi.org/10.1038/d41586-019-01234-2>
- [29] E. Patterson and D. J. Eatough, "Indoor/outdoor relationships for ambient pm2.5 and associated pollutants: epidemiological implications in linden, utah," *Journal of the Air & Waste Management Association*, vol. 50, no. 1, pp. 103–110, 2000.
- [30] D. Y. Pui, S.-C. Chen, and Z. Zuo, "Pm2.5 in china: Measurements, sources, visibility and health effects, and mitigation," *Particuology*, vol. 13, pp. 1–26, 2014.
- [31] EPA, *Air quality guidelines: global update 2005: particulate matter, ozone, nitrogen dioxide, and sulfur dioxide*. World Health Organization, 2006.
- [32] N. P. Service, "Climate change," 2022. [Online]. Available: <https://www.nps.gov/jotr/learn/nature/climate-change.htm>
- [33] J. Prophet, Y. M. Kow, and M. Hurry, "Cultivating environmental awareness: Modeling air quality data via augmented reality miniature trees," in *International Conference on Augmented Cognition*. Springer, 2018, pp. 406–424.
- [34] K. Bickerstaff and G. Walker, "Clearing the smog? public responses to air-quality information," *Local environment*, vol. 4, no. 3, pp. 279–294, 1999.
- [35] R. Lu and R. P. Turco, "Ozone distributions over the los angeles basin: Three-dimensional simulations with the smog model," *Atmospheric Environment*, vol. 30, no. 24, pp. 4155–4176, 1996.
- [36] C. Haerberling, "Cartographic design principles for 3d maps—a contribution to cartographic theory," in *Proceedings of ICA Congress Mapping Approaches into a Changing World*, 2005.
- [37] W. Zhu, N. Yao, Q. Guo, and F. Wang, "Public risk perception and willingness to mitigate climate change: city smog as an example," *Environmental Geochemistry and Health*, vol. 42, no. 3, pp. 881–893, 2020.
- [38] U. EPA, "Air quality index: a guide to air quality and your health," Washington, DC, US Environmental Protection Agency, 2003.
- [39] Y. Wu, L. Zhang, J. Wang, and Y. Mou, "Communicating air quality index information: Effects of different styles on individuals' risk perception and precaution intention," *International journal of environmental research and public health*, vol. 18, no. 19, p. 10542, 2021.
- [40] N. P. Service, "Ocotillo patch," 2022. [Online]. Available: <https://www.nps.gov/places/ocotillo-patch.htm>
- [41] G. Earth, "Measure distance elevation," 2022. [Online]. Available: <https://support.google.com/earth/answer/148134?hl=en>
- [42] K. L. El-Ashrawy, "Investigation of the accuracy of google earth elevation data," *Artificial Satellites*, vol. 51, no. 3, p. 89, 2016.
- [43] H. Tamiminia, B. Salehi, M. Mahdianpari, L. Quackenbush, S. Adeli, and B. Brisco, "Google earth engine for geo-big data applications: A meta-analysis and systematic review," *ISPRS Journal of Photogrammetry and Remote Sensing*, vol. 164, pp. 152–170, 2020.
- [44] "Official x3dom documentation," 2022. [Online]. Available: <https://doc.x3dom.org/>
- [45] "Arcgis pro," 2022. [Online]. Available: <https://pro.arcgis.com/>
- [46] Domlysz, "Blendergis," 2022. [Online]. Available: <https://github.com/domlysz/BlenderGIS>
- [47] I.-K. Kim, H.-W. Jang, K.-H. Yoo, and J.-S. Ha, "Specification and implementation of projective texturing node in x3d," *International Journal of Contents*, vol. 12, no. 2, pp. 1–5, 2016.
- [48] M. Kamburelis, "Shadow maps and projective texturing in x3d," in *Proceedings of the 15th International Conference on Web 3D Technology*, 2010, pp. 17–26.
- [49] C. Everitt, "Projective texture mapping," *White paper, NVidia Corporation*, vol. 4, no. 3, 2001.
- [50] N. Ngo, S. Kokoyo, and J. Klopp, "Why participation matters for air quality studies: risk perceptions, understandings of air pollution and mobilization in a poor neighborhood in nairobi, kenya," *Public Health*, vol. 142, pp. 177–185, 2017.
- [51] S. Gota, H. G. Fabian, A. A. Mejia, and S. S. Punte, "Walkability surveys in asian cities," *Clean Air Initiative for Asian Cities (CAI-Asia)*, vol. 20, pp. 2017–2021, 2010.
- [52] T. Kimura, T. Nose, S. Hirooka, Y. Chiba, and A. Ito, "Comparison of speech recognition performance between kald and google cloud speech api," in *International Conference on Intelligent Information Hiding and Multimedia Signal Processing*. Springer, 2018, pp. 109–115.
- [53] S. Jasanoff, "The political science of risk perception," *Reliability Engineering & System Safety*, vol. 59, no. 1, pp. 91–99, 1998.
- [54] K. Bickerstaff, "Risk perception research: socio-cultural perspectives on the public experience of air pollution," *Environment international*, vol. 30, no. 6, pp. 827–840, 2004.